

A CFD based investigation for Evaluation of Unsteady Hydrodynamic Coefficients of 3D fin in viscous flow.

Zulfiqar Nazir, SU Yumin

College of Shipbuilding Engineering, Harbin Engineering University, Harbin 150001, China

Abstract: The study of fin and control surfaces of underwater vehicle moving in a fluid is an interesting and challenging research subject in the field of underwater locomotion and propulsion for underwater vehicle. Typically the effect of Fin oscillation on fluid flow around such a body is highly unsteady, generating vortices and requiring detailed analysis of fluid-structure interactions. An understanding of the complexities of such flows is of interest to engineers interested in developing vehicles capable of emulating the high dynamic performance of propulsion and maneuvering. In the present study, a CFD based RANS simulation of 3D fin body moving in the viscous fluid has been developed to completely investigate its hydrodynamic performance by evaluating the hydrodynamic coefficients (lift, drag and moment) at two different oscillations frequencies. In this simulation, an implicit pressure-based finite volume method is used for time independent accurate computation of incompressible flow using second order accurate convective flux discretisation schemes. A parametric analysis of the factors that affect the hydrodynamic performance of the fin body is presented, along with the comparison of results with the experimental data.

Key Words: 3D Fin, CFD, RANS, Hydrodynamic Coefficients, Unsteady.

1. Introduction

The development of autonomous underwater vehicles has progressed quite significantly in the past decade due in large part to the increasing interest in unmanned underwater surveillance and monitoring. An approach that has shown promise for design of vehicles suitable to such environments is to draw from nature, both vehicle morphology and methods of locomotion. The study of underwater locomotion has long been a subject of interest to the biological

community^[1-6]. Many researchers have drawn an inspiration from bio-locomotion and biomimetics in attempt to design the underwater vehicle having shape similar to the fish like bodies^[7], to improve its hydrodynamic performance and stability. A large portion of the work that has been performed relative to swimming vehicles has focused on the task of forward locomotion^[8-14]. The stability and maneuvering of underwater vehicle either propelled or autonomous is directly related with the fin and control surfaces of the underwater

vehicle, which are the fundamental of dynamics and control of underwater vehicle. In past lot of work is done for the optimization^[15] and designing of 3D Fin from 2D foil shapes^[16] however very less quantitative research is available on the evaluation of hydrodynamic coefficients of 3D fin in interaction with the viscous flow. The two most important hydrodynamic quantities affecting the performance of underwater vehicle are lift and drag associated with the fin surfaces of such underwater vehicle. Nearly all hydrodynamic analysis is an attempt to maximize the lift for a given amount of drag, or conversely to minimize the drag for a given amount of lift. The analysis of these quantities for various UWV fins configurations forms the basis of most hydrodynamic research. Because of this, reliable methods to compute these forces from available experimental or computational data are essential. Traditionally, hydrodynamic forces have been measured in towing tanks using strain-gauge balances. This approach is very good for measuring the lift, but the drag of a typical fin surfaces at reasonable angles of incidence is often an order of magnitude less than the lift, and therefore, more difficult to measure. In particular, the presence of the model sting or support makes accurate drag measurement very difficult using this approach. The present work represents the detail study of 3D Fin which is moving in the viscous flow and whose hydrodynamic performance is evaluated for unsteady flow conditions. The families of airfoils known as the NACA 4-series^[17] and 6-series^[17-18] are the standard 2D surfaces being utilized for the designing and construction of 3D lifting objects such as hydroplanes, propellers and rudders. Regardless of

the type of lifting surface, its hydrodynamic characteristics will strongly be affected by the shape of the fin section^[18]. A convenient way of describing the hydrodynamic characteristics of fin is to plot the values of the hydrodynamic coefficients against the angle of attack. A measure of the efficiency of the fin as a lifting surface is given by the lift-drag ratio. This ratio increases from zero at zero lift to a maximum value at a moderate lift coefficient, after which it decreases relatively slowly as the angle of attack is further increased. It is desirable for the fin to have the smallest possible drag and maximum lift coefficient for high and moderate speed. Keeping in view all above factors experimental model was designed and constructed utilizing the NACA 0018 foil surface with the surface area is 400 mm, $\theta = 10$ Degrees, spanwise distance $L = 400$ mm and all the chordwise distances are in mm as narrated through table 1 and Fig 1. Series of experiments^[19] were conducted at the towing tank facility of HEU for the evaluation of hydrodynamic coefficients of 3D fin for the steady and unsteady state conditions with Reynolds number 8.75×10^5 , kinematic viscosity 0.001003 kg/m.sec and density 998.2 kg/m³, which are used in the present work for comparison with the simulated results.

br	bt	bc	Lo/br	Lc/bc	bt/br
493.8	306.2	400	0.267	0.224	0.62

Table 1: Parameters of Experimental model.

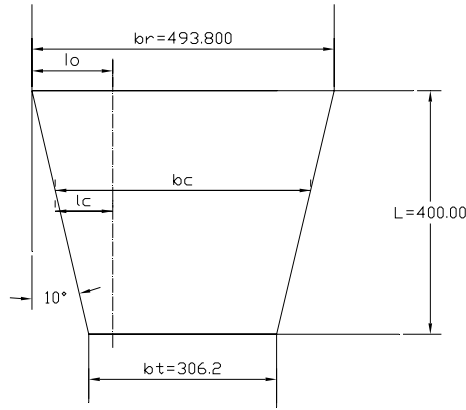


Figure 1: Dimensional Details of experimental model.

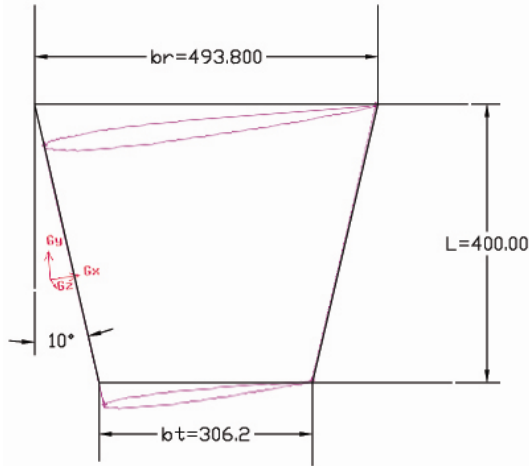


Figure 2: Designed and Experimental Model Dimension equality.

2. Unsteady State Analyses

In case of unsteady state simulation the choice of grid around the fin body is limited to the unstructured grid scheme so as to utilize the dynamic mesh option, keeping in view the above limitation unstructured grid is generated by using tetrahedral cells as basic grid elements. One of the important factors in unsteady

state simulation is the oscillating motion of the body whose hydrodynamic performance is under evaluation, which in case of present simulation is the 3D fin body placed in control volume domain and which is to be oscillated separately for two different frequencies. In case of FLUENT that can be achieved the by an efficient compiled UDF. The accurate compilation of UDF keeping in view the experimental scenario will yield the solution as close as possible to the experimental.

2.1 Turbulent model and boundary conditions.

A computational system based on a method of 3D Navier-Stokes equations solver is developed and can be directly applied to realistic hydrodynamic problems. For the three dimensional problem of a moving fin in viscous fluid, the turbulent flow can be characterized by fluctuating velocity fields. These fluctuations mix transported quantities can cause the transported quantities to fluctuate as well. Since these fluctuations can be of small scale and high frequency, they are too computationally expensive to simulate directly in practical engineering calculations. Instead, the solution variables in the instantaneous (exact) Navier-Stokes (NS) equations based on CFD code description ^[20] can be decomposed into the mean and fluctuating components by the Reynolds-averaged approach, resulting in a modified set of equations that are computationally less expensive to solve. In the simulations the boundary conditions consisted of a pressure outlet with backflow direction normal to boundary, and a no-slip wall condition at

the fin body surface with wall constant as 0.5 which is the default value set by FLUENT. Top and bottom faces of controlled volume are defined as symmetry. Free stream velocity which is in opposite direction to the x-axis is defined by the means of velocity components option keeping the magnitude normal to the boundary, where as in the case of left and right velocity inlets the components of velocity are defined by the components option where x-component is defined as the 2.198 m/s.

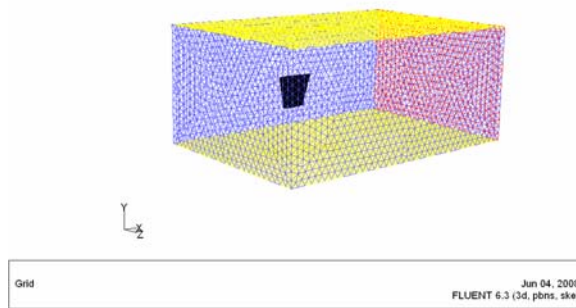


Figure 3: View of Boundary conditions.

2.2 Mesh Structure and Moving mesh.

In the present simulation an unstructured tetrahedral grid, as shown in Fig 4, which was generated for the three-dimensional geometry is implemented. The domain contains a single unstructured grid around the 3D fin body and the grid points are placed in the flow field in a very irregular fashion. Because there is no regularity in the mesh, there are no coordinate lines.

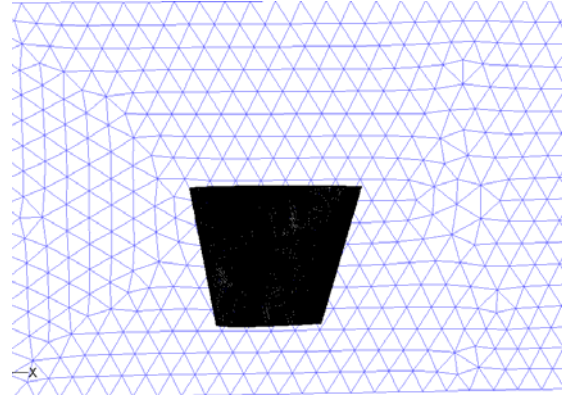


Figure 4: Unstructured Tetrahedral Grid.

In the process of creating a grid interface, the code creates a non-conformal grid interface between deforming walls. It has been found that there is no need to implement the grid interfaces functionality available in the FLUENT code. The numerical algorithm automatically updates the mesh after each time step relative to the 3D fin motion using a number of meshing tools [20] such as “Dynamic layering”, “Spring-based smoothing” and “Local remeshing”. To smooth the mesh, a value of 1 is used for the boundary node relaxation and a standard value of 0.001 is used for the convergence tolerance and the Spring Constant Factor 0.05. Under remeshing the “must improve skewness” option was selected in the dynamic mesh parameters, this is because by default FLUENT replaces the agglomerated cells only if the quality of the remesh has improved. A zero value is specified for the minimum length scale which specifies the lower limit of cell size below which the cells are marked for remeshing and 1000 for the maximum length scale which specifies the upper limit of cell size above which the cells are marked for remeshing and 0.8 for the maximum cell skewness. These values are selected

based on the original mesh scale information, if a cell exceeds these limits the cell is marked for remeshing.

2.3 User Defined Function

The motion of the Fin is described in the present Simulation using a FLUENT user-defined function (UDF) which is dynamically loaded with the FLUENT solver to enhance the standard features of the code. Although a wide range of applications can be addressed using UDFs in FLUENT, not all solution variables such as specific heat values can be accessed in this manner. In the present simulation a dynamic mesh UDF is implemented using the DEFINE macro DEFINE-CG-MOTION. The function is only executed as a complied UDF and cannot be executed as an interpreted UDF. The Fin user-defined function was executed as a complied UDF in a two-step process, first building and then loading the shared library object file from the source code using the graphical user interface.

2.4 Results and Discussions.

Lift coefficient is observed along the z-axis and drag coefficient along the x-axis. Moment axis is established about the fin body at y axis. The moment coefficient about this axis also termed as pivot axis will be the same at all the points lying on the axis. The coordinates of these points are the moment centre coordinates ($X = -0.918$, $Y = 0, 0.1, 0.2, 0.3, -0.1, -0.2$, $Z = 0$), utilized for calculation of moment coefficient, x and z coordinates are fixed only y coordinate is having variable magnitude as shown in Fig 5.

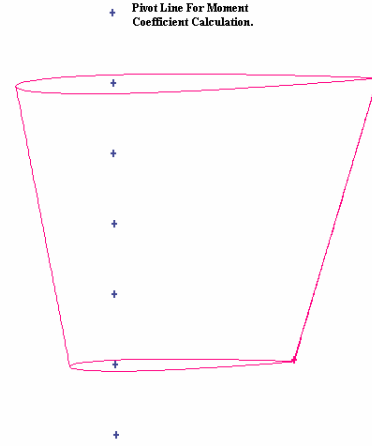


Figure 5: View of Moment axis.

For evaluation of unsteady state hydrodynamic performance of 3D fin CFD Simulated model is calculated separately for two separate oscillation frequencies $T = 4.5$ s and $T = 5.298$ s keeping in view the Availability of experimental data. Apart from following the fluent convergence criteria for time dependent calculations ^[20] both the simulations are computed for more then three cycles so as to find consistency and stability in the simulated results by comparing the individual values of hydrodynamic coefficients at various values of attack angle in successive cycles which will yield an accurate solution, later to be utilized for successful comparison with the experimental data. Statistical simulated data reveals that for small values of attack angle simulation results are having very less percentage difference as compared with the experimental data but however with the increase in attack angle the percentage difference also increases upto some extent and with further increase it is found to be constant. As we move close to the stall point ^[16] which is falling at 31.678 degrees percentage difference is found to be 19-21% for lift coefficient and that of 15-19% for drag coefficient In general both

the simulated results are found in close agreement with the experimental as narrated through graphical Fig 6-13 drawn between the hydrodynamic coefficients and attack angle. Further the impact of the fin oscillation in interaction with the surrounding viscous flow is also explained in terms of dynamic and static pressure contours on the complete fin body as shown in Fig 14-15 which itself dictates the verification of Bernoulli's principle, greater the velocity of flow in a fluid, greater the dynamic pressure and the less the static pressure.

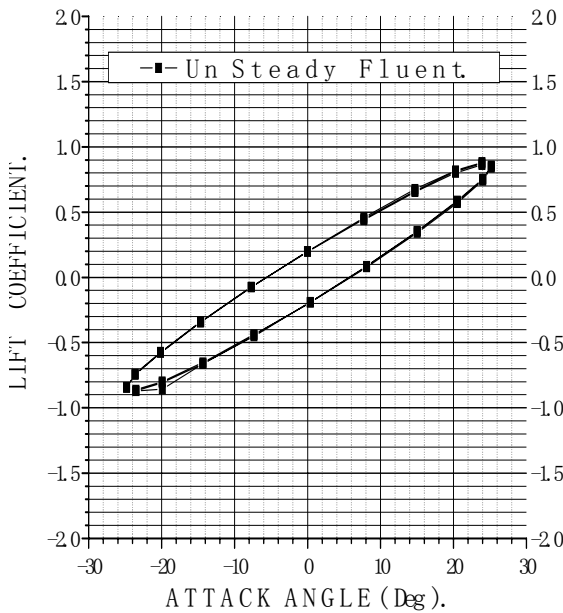


Figure 6: Unsteady State Analyses Lift Coefficient T = 4.5 Seconds – Fluent.

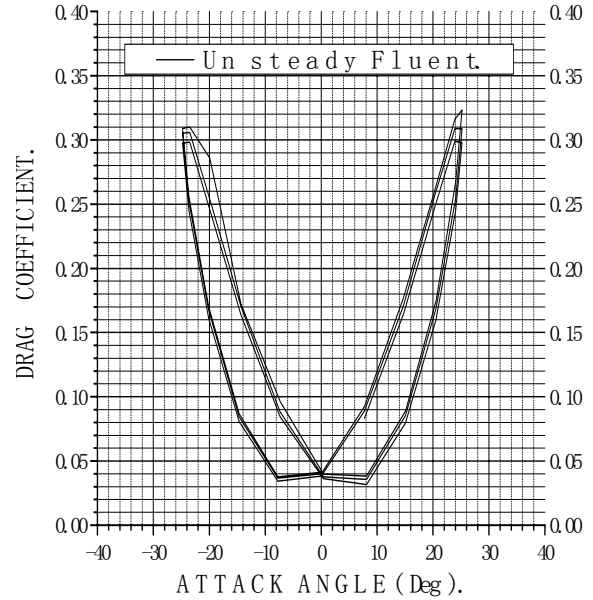


Figure 7: Unsteady State Analyses Drag Coefficient T = 4.5 Seconds – Fluent.

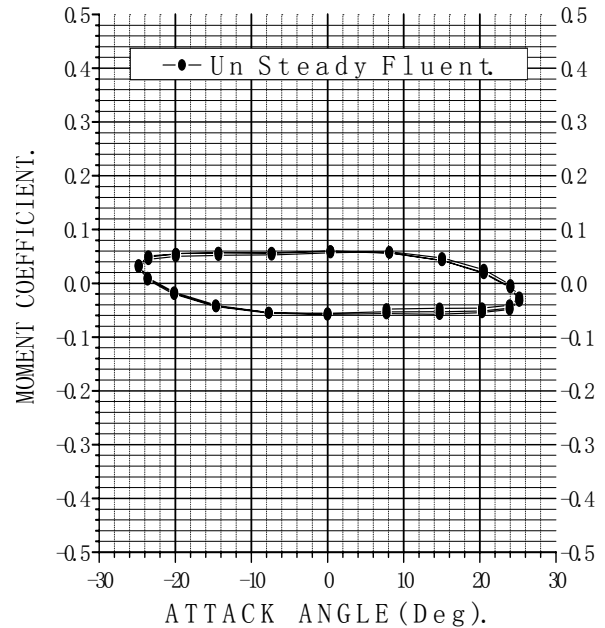


Figure 8: Unsteady State Analyses Moment Coefficient T = 4.5 Seconds – Fluent.

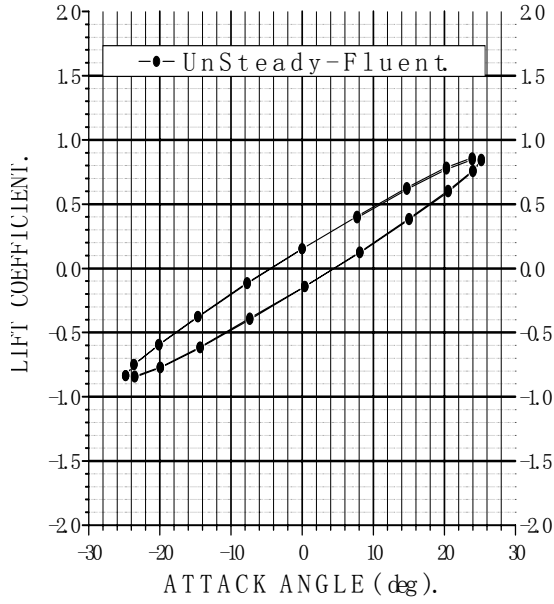


Figure 9: Unsteady State Analyses Lift Coefficient T = 5.298 Seconds – Fluent.

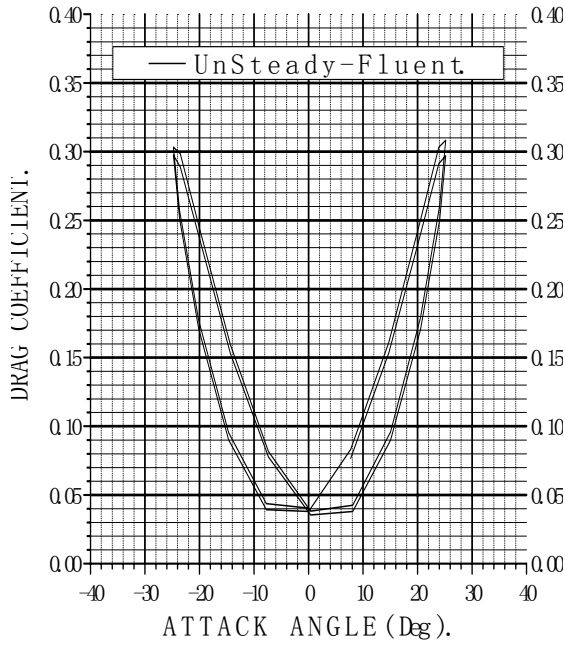


Figure 10: Unsteady State Analyses Drag Coefficient T = 5.298 Seconds – Fluent.

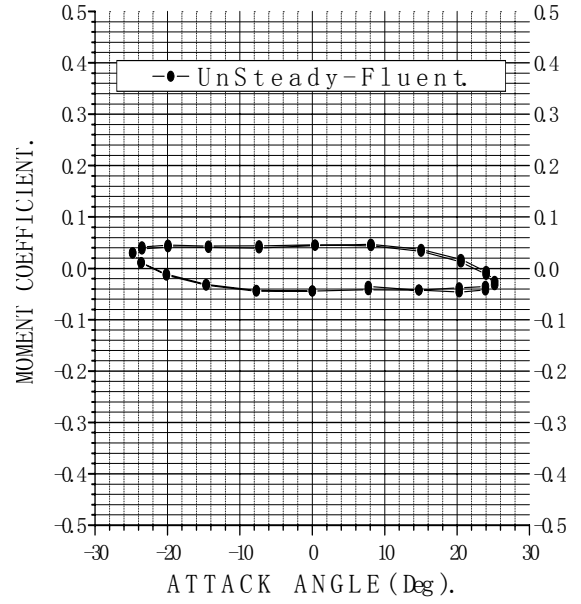


Figure 11: Unsteady State Analyses Moment Coefficient T = 5.298 Seconds – Fluent.

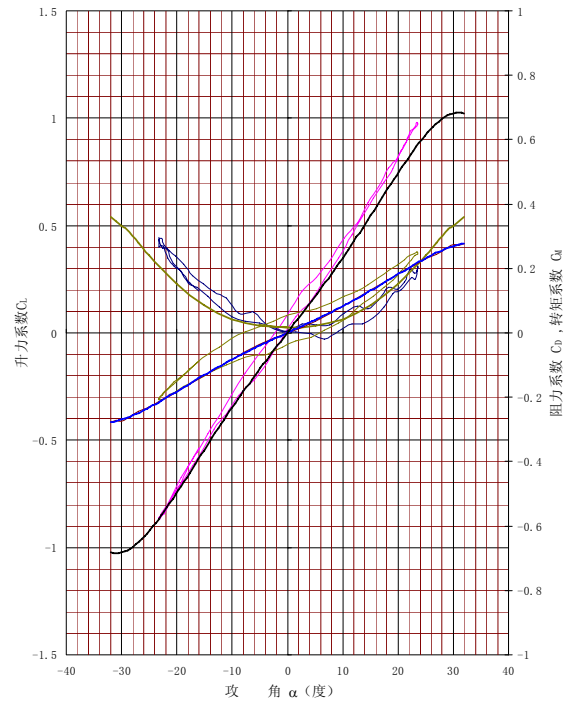


Figure 12: Steady and unsteady experimental results T = 5.298 Seconds.

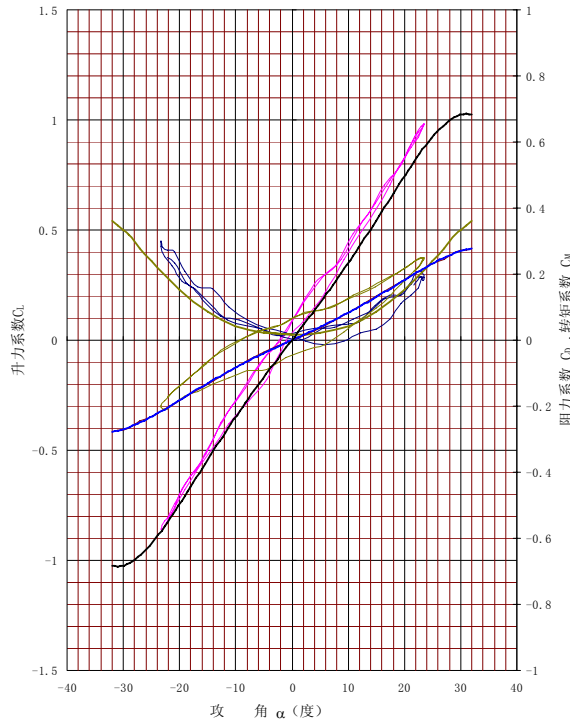


Figure 13: Steady and unsteady experimental results $T = 4.5$ Seconds.

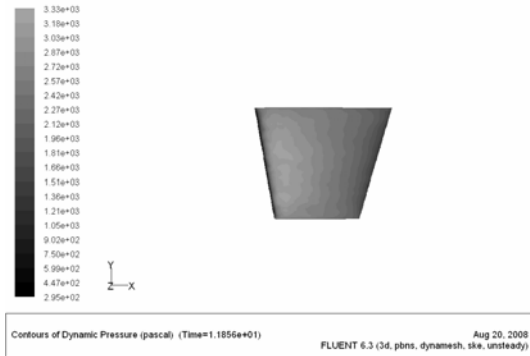


Figure 14: Contours of dynamic pressure $T = 5.298$ Seconds.

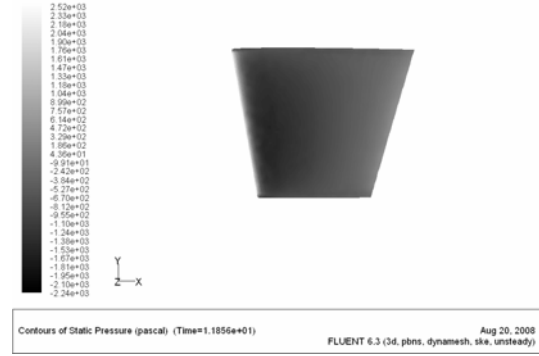


Figure 15: Contours of static pressure $T = 5.298$ Seconds.

3. Conclusion.

The work in this paper has addressed the evaluation of unsteady hydrodynamic coefficients of 3D fin in interaction with viscous flow. CFD based simulations have been performed separately for two oscillation frequency to validate the present method with the experimental results. The results of both the simulations are found in close agreement with the experimental results and hence validating the present simulated work as an effective tool for evaluation of unsteady hydrodynamic coefficients of 3D fin which can be further be taken up for analyses of stability and maneuvering of fin actuated underwater vehicles.

References

- [1] S. Childress, Mechanics of swimming and flying. Cambridge: Cambridge University Press, 1981.
- [2] J. Lighthill, Mathematical Bio fluid dynamics. Philadelphia: SIAM, 1975.

- [3] J. Newman and T. Wu, "Hydrodynamical aspects of fish swimming, in *Swimming and Flying in Nature*", Vol 2. T. Wu, C. Brokaw, and C. Brennen, Eds. New York: Plenum Press, 1975, pp. 615–34.
- [4] D. Weihs, "A hydrodynamical analysis of fish turning maneuvers," *Proc. R. Soc. Lond. B*, vol. 182, pp. 59–72, 1972.
- [5] I. Spierts and J. van Leeuwen, "Kinematics and muscle dynamics of C- and S-starts of carp (*Cyprinus carpio* L.)," *J. Exp. Biology*, vol. 202, pp. 393–406, 1999.
- [6] P. Domenici and R. Blake, "The kinematics and performance of fish fast-start swimming," *J. Exp. Biology*, vol. 200, pp. 1165–1178, 1997.
- [7] Kristi A. Morgansen, Timothy M. La Fond, and Jennifer X. Zhang "Agile maneuvering of fin actuated under water vehicle".
- [8] D. Barrett, M. Grosenbaugh, and M. Triantafyllou, "The optimal control of a flexible hull robotic undersea vehicle propelled by an oscillating foil," in *Proc. 1996 Symp. Aut. Underwater Veh. Tech.*, 1996, pp. 1–9.
- [9] K. Morgansen, V. Duindam, R. Mason, J. Burdick, and R. Murray, "Nonlinear control methods for planar carangiform robot fish locomotion," in *Proc. IEEE Int. Conf. Rob. Aut.* 2001.
- [10] P. Vela, K. Morgansen, and J. Burdick, "Second order averaging methods for oscillatory control of under actuated mechanical systems," 2002, to appear in *Proceedings of the 2002 American Control Conference*.
- [11] S. Saimek and P. Li, "Motion planning and control of a swimming Machine," in *Proc. Amer. Contr. Conf.*, 2001, pp. 125–30.
- [12] R. Mason and J. Burdick, "Propulsion and control of deformable bodies in an ideal fluid," in *Proc. IEEE Int. Conf. Rob. Aut.* 1999, pp. 773–80.
- [13] S. Kelly, R. Mason, C. Anhalt, R. Murray, and J. Burdick, "Modeling and experimental investigation of carangiform locomotion for control," in *Proc. Amer. Contr. Conf.*, 1998, pp. 1271–6.
- [14] J. Liu, I. Dukes, R. Knight, and H. Hu, "Development of fish-like swimming behaviors for an autonomous robotic fish," in *Proceedings of the Control'04*. University of Bath, England: IEE, September 2004, ID217.
- [15] Wenbin Song, Andy Keane, Hakki Eres, Graeme Pound, and Simon Cox "Two Dimensional Airfoil optimization Using CFD in a Grid Computing Environment" School of Engineering Sciences University of Southampton Highfield, Southampton, SO17 1BJ, UK.
- [16] Dave Carswell and Nick Lavery "3D solid fin model construction from 2D shapes using non-uniform rational B-spline surfaces" Materials Research Centre, University of Wales Swansea, Singleton Park, Swansea SA2 8PP, United Kingdom.
- [17] Abbott IH, Doenhoff AEv, Stivers LS. Summary of airfoil data, National Advisory Committee for Aeronautics 824, 1945.
- [18] Jacobs EN. Preliminary report on laminar-flow airfoils and new methods adopted for airfoil and boundary-layer investigations. NACA WR L-345, 1939.
- [19] Tong Zhen-Ming, Zhao Xiao-dong, and Ding Yong. Series experiments of steady and unsteady 3D hydrofoil, research report of HEU 2004.
- [20] Fluent Tutorials.